

THE CHARGED KAON PRODUCTION IN  $^{58}\text{Ni}$   
ON  $^{58}\text{Ni}$  COLLISIONS AT 1.93 A GeV\* \*\*

M. KIREJCZYK

Institute of Experimental Physics, Warsaw University  
Hoża 69, 00-681 Warsaw, Poland  
for the FOPI collaboration

*(Received November 24, 1997)*

The production of charged kaons in the central  $^{58}\text{Ni}+^{58}\text{Ni}$  reactions at 1.93 A GeV was studied with the FOPI spectrometer. A brief description of the apparatus is provided. The particle identification procedure is described. Two examples of obtained results are discussed.

PACS numbers: 25.75. -q, 25.75. Dw

The role of kaons as probes of possible chiral symmetry restoration, and messengers from the hot and compressed reaction zone has been discussed elsewhere [1]. The kaon production is especially interesting in reactions at bombarding energies between 1 and 2 A GeV. In this energy range kaons are produced sub- or near-threshold, and they are sensitive to the conditions in the central reaction zone. Unfortunately, there is no unambiguous interpretation of the experimental results obtained so far. This is due to a large number of free parameters and approximations contained in all theories aiming to describe the dynamics of heavy ion collisions. It is therefore necessary to conduct a complex set of measurements, of many quantities, using different systems at a number of energies in order to clarify this situation.

### 1. The detector

The FOPI detector at SIS accelerator in GSI Darmstadt is a close-to  $4\pi$  charged particle spectrometer [2]. Forward angles ( $1^\circ < \theta_{\text{lab}} < 30^\circ$ ) are covered by the Forward Wall Detector (scintillators measuring energy

---

\* Presented at the XXV Mazurian Lakes School of Physics, Piaski, Poland, August 27–September 6, 1997.

\*\* This work was in part supported by the Polish Committee of Scientific Research (KBN) under grants nr. 2 P03B 019 11 and 2P032 1104.

loss and time of flight, used also as a multiplicity trigger) and the Helitron drift chamber. Backward angles ( $\theta_{\text{lab}} > 30^\circ$ ) are covered by the Central Drift Chamber (CDC), which is supplemented (for  $\theta_{\text{lab}} > 40^\circ$ ) by the Barrel (scintillators for time of flight measurement). Both drift chambers and the Barrel are placed inside a superconducting solenoid.

It should be noted, that during the experiment described here, the Helitron was not fully operational yet, therefore the results presented were obtained with the CDC and the Barrel only.

## 2. Identification procedure

Drift chambers measure the curvature of particle tracks, energy loss and emission angles, which allows to calculate the momentum to charge ratio ( $p/q$ ) and the specific energy loss ( $dE/dx$ ). When time of flight is taken into account, velocity can be calculated in addition. Combining  $dE/dx$  with velocity makes possible the charge determination, while combining any of those two quantities with  $p/q$  allows one to obtain, in 2 semi-independent ways, the mass. Procedures that use  $dE/dx$  rely on the Bethe–Bloch formula.

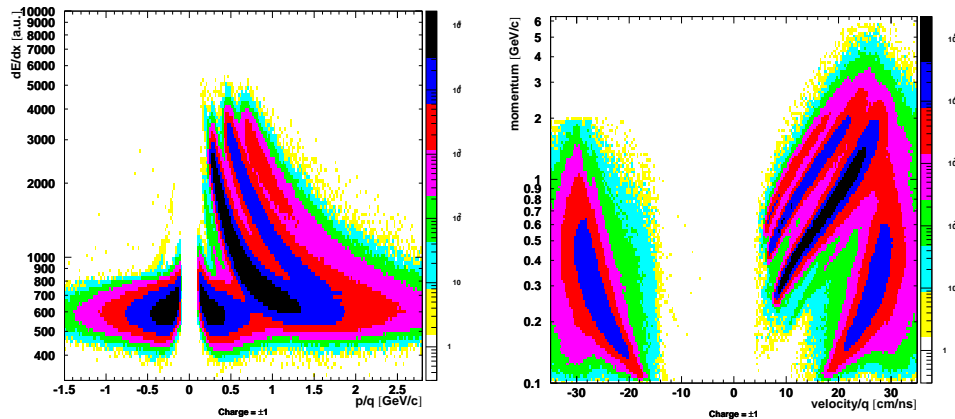


Fig. 1. Illustrations of two mass identification methods

On figure 1 two distributions, illustrating two methods of mass determination, are shown. The left one shows the specific energy loss plotted versus momentum, the right one shows momentum plotted versus velocity. For both distributions only particles with charge  $\pm 1$  were selected. Note, that the quantity plotted on the horizontal axis is always divided by the charge, so negatively charged particles appear on the left-hand side of the plots. The ridges, that are visible on both plots correspond to (from left to right):  $K^-$ ,  $\pi^-$ ,  $\pi^+$ ,  $K^+$ , protons, deuterons and tritons on the left plot, and

respectively  $\pi^-$ , tritons, deuterons, protons,  $K^+$ , and  $\pi^+$  on the right plot ( $K^-$  line is not visible).

In the first method  $\pi^+$  mesons are indistinguishable from protons for momenta above ca. 650 MeV/c. This is caused by the non-monotonic behaviour of the Bethe–Bloch curves. In addition, for the same reason, the mass assignment is inherently ambiguous (most points can be assigned two values of mass parameter, one corresponding to a Bethe–Bloch line that is raising at that point, and the other parameter corresponding to a line that is falling there). The  $K^+$  identification is limited to particles with momenta below about 350 MeV/c. On the other hand this method uses information drawn only from the CDC, so there are no problems of combining data from different detectors. For the second method, the “abundant” particles are separated almost in the whole momentum range, and the  $K^+$  identification limit is raised to about 550 MeV/c.

A comparison of both methods is shown in the figure 2. A CDC mass (obtained via the first method) is plotted versus barrel mass (obtained via the second method). The plot shows, that in order to enhance the kaon separation both methods should be combined with an additional cut placed on the mass difference. The small structures corresponding to particles identified as pions via CDC mass, and protons or deuterons via barrel mass, are caused by erroneous matching of data registered in CDC and Barrel. Under the conditions that were in place during that experiment their number is negligibly small (the z- or colour axis is logarithmic).

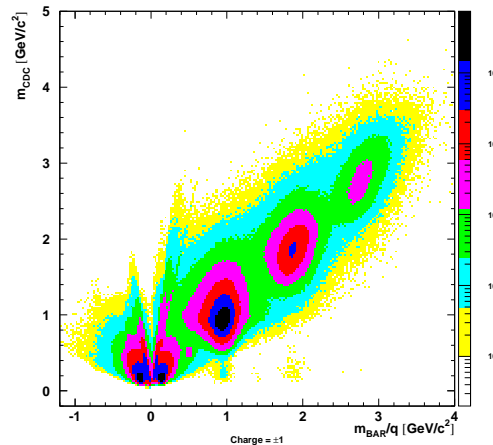


Fig. 2. Masses obtained with two identification methods plotted one against the other.

A spectrum of the average mass is shown on the figure 3. There were additional cuts used here in order to allow for a clear distinction of  $K^-$ . The main cut was applied to momentum ( $p < 400$  MeV/c). The cuts on the specific energy loss and velocity were chosen in such a way, that the momentum cut was the only one that was significantly reducing number of kaons. Due to much higher statistics,  $K^+$  mesons can be separated up to momenta of 600 MeV/c. There is also a perpendicular momentum cut applied, which is caused by the non-zero radius of the Barrel. A minimum  $p_t$  of ca. 110 MeV/c is required for any charge 1 particle to reach the Barrel and be registered there.

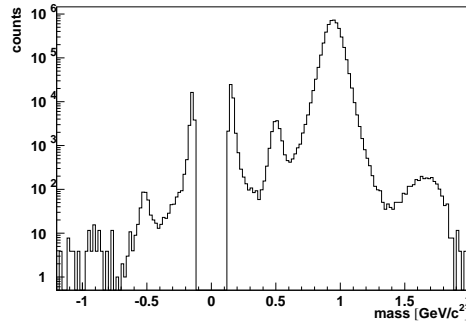


Fig. 3. Average mass spectrum

### 3. Sample results

One of the interesting kaonic observables is a so-called flow pattern, which is defined here to be the behaviour of average in-plane momentum ( $\langle p_x \rangle$ ) as a function of scaled rapidity ( $y^0$ ).

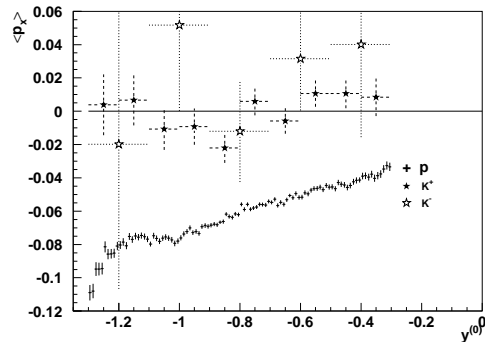


Fig. 4. Flow pattern

The flow patterns for protons,  $K^+$  and  $K^-$  mesons are shown in figure 4. The  $K^+$  mesons seem not to show significant deviation from 0, and this is a noteworthy conclusion. According to theoretical calculations it may prove (depending on the model) either the presence of a weakly repulsive kaon potential, which must consist of strong scalar (attractive) and vector (repulsive) potentials almost cancelling each other [3], or the importance of taking kaon rescattering inside the nuclear medium into proper consideration [4]. Unfortunately, the error bars on the  $K^-$  points are too large to draw similarly significant conclusions.

Another characteristics that has been looked at is the so-called Boltzmann spectrum. It is the weighted (with  $1/m_t^2$ ) spectrum of perpendicular mass ( $m_t = \sqrt{m^2 c^2 + p_t^2}/c$ ). If the emitted particles follow the Boltzmann–Maxwell distribution, or if the emission pattern may be characterized as a combination of thermal motion and radial blast, such a spectrum (for a small rapidity slice) is a single exponent [5]. The interest in those spectra has been sparked by the success of the thermal model in describing many features of particle emission patterns (for instance [6]). In addition, if particles conform to the thermal distribution, the extrapolation to the phase space not covered by the detector becomes quite easy. An example of such a plot is shown in figure 5, for the scaled rapidity slice between -0.8 and -1. The quality of the single exponent fit is pretty good.

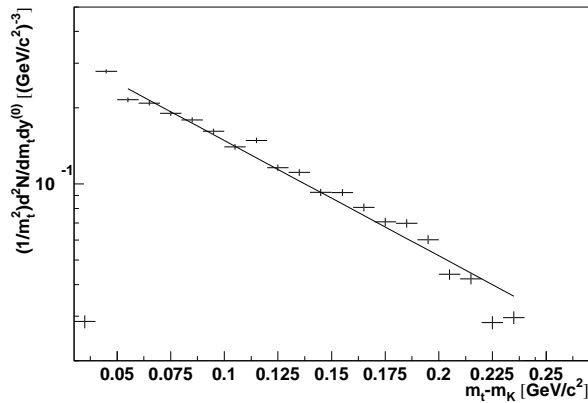


Fig. 5. Boltzmann spectrum of  $K^+$  for  $-1.0 < y^{(0)} < -0.8$ .

## REFERENCES

- [1] P. Senger, *Acta Phys. Pol.*, **B29**, 273 (1998).
- [2] J. Ritman, *Nucl. Phys.* **B44**, 708 (1995).
- [3] G.Q. Li, C.M. Ko, *Nucl. Phys.* **A594**, 460 (1995).
- [4] C. David *et al.*, submitted to *Acta Phys. Pol.* **A**, nucl-th/9611016.
- [5] P. Siemens, J. Rassmussen, *Phys. Rev. Lett.* **42**, 888 (1979).
- [6] P. Braun–Munzinger *et al.*, *Phys. Lett.* **B344**, 43 (1995); *Phys. Lett.*, 1 **B356** (1996).